

Contribution of serine racemase/D-serine pathway to neuronal apoptosis

Simona Esposito,¹ Andrea Pristerà,¹ Giovanna Maresca,¹ Sebastiano Cavallaro,² Armando Felsani,¹ Fulvio Florenzano,³ Luigi Manni,⁴ Maria T. Ciotti,¹ Loredano Pollegioni,⁵ Tiziana Borsello⁶ and Nadia Canu^{1,7}

¹Istituto di Biologia Cellulare e Neurobiologia, CNR, Roma, Italy

²Istituto di Scienze Neurologiche, Centro di Genomica Funzionale, CNR, Catania, Italy

³Fondazione Santa Lucia and European Brain Research Institute, Roma, Italy

⁴Istituto di Farmacologia Traslazionale, CNR, Roma, Italy

⁵Dipartimento di Biotecnologie e Scienze della Vita, Università degli Studi dell'Insubria, Varese, Italy

⁶Istituto di Ricerche Farmacologiche Mario Negri, Milano, Italy

⁷Dipartimento di Neuroscienze, Università di Tor Vergata, Roma, Italy

Summary

Recent data indicate that age-related N-methyl-D-aspartate receptor (NMDAR) transmission impairment is correlated with the reduction in serine racemase (SR) expression and D-serine content. As apoptosis is associated with several diseases and conditions that generally occur with age, we investigated the modulation of SR/D-serine pathway during neuronal apoptosis and its impact on survival. We found that in cerebellar granule neurons (CGNs), undergoing apoptosis SR/D-serine pathway is crucially regulated. In the early phase of apoptosis, the expression of SR is reduced, both at the protein and RNA level through pathways, upstream of caspase activation, involving ubiquitin proteasome system (UPS) and c-Jun N-terminal kinases (JNKs). Forced expression of SR, together with treatment with NMDA and D-serine, blocks neuronal death, whereas pharmacological inhibition and Sh-RNA-mediated suppression of endogenous SR exacerbate neuronal death. In the late phase of apoptosis, the increased expression of SR contribute to the last, NMDAR-mediated, wave of cell death. These findings are relevant to our understanding of neuronal apoptosis and NMDAR activity regulation, raising further questions as to the role of SR/D-serine in those neuro-pathophysiological processes, such as aging and neurodegenerative diseases characterized by a convergence of apoptotic mechanisms and NMDAR dysfunction.

Key words: neuronal death; proteasome; c-Jun N-terminal Kinase; D-serine; NMDA receptor; serine-racemase; cerebellar granule neurons; apoptosis.

Introduction

Physiological NMDAR activation generates signals that play an important role in development, survival, and synaptic plasticity, while its excessive stimulation results in excitotoxic cell death (Hardingham, 2006; Hetman & Kharebava, 2006). During nervous system development, NMDAR activation exerts a trophic action in different neuronal populations (Monti &

Contestabile, 2000). In particular, it plays a critical role in cerebellar granule neurons (CGN) apoptosis during the first week of cerebellar development. Cerebellar granule neurons are generated in the external granule layer and migrate to the internal granule (Ryder & Cepko, 1994). During their postnatal migration, CGNs require excitatory inputs from the glutamatergic mossy fibers for proper differentiation and development; otherwise, they die by apoptosis (Burgoyne & Cambray-Deakin, 1988). This condition can be mimicked *in vitro* in primary cultures of CGNs. Indeed, CGNs undergo spontaneous cell death when they grow in a medium containing physiological potassium concentration (5 mM KCl). This neuronal death occurs by a sequence of apoptosis–autophagy and necrosis phenomena and is hampered when neurons are grown in medium containing depolarizing levels of potassium (25 mM KCl) or moderate concentration of NMDA. It is assumed that both factors, through different signal transduction pathways, mimic the pro-survival electrical stimulation from afferent synapses (Gallo *et al.*, 1987; D'Mello *et al.*, 1993; Nardi *et al.*, 1997; Xifro *et al.*, 2005). NMDAR-mediated pro-survival activity is, in part, mediated through the activation of PI3K and MAPK pathways (Zhang *et al.*, 1998; Hetman & Kharebava, 2006).

NMDAR is activated by the neurotransmitter glutamate as well as by a second agonist acting at the strychnine-insensitive site of glycine (Johnson & Ascher, 1990). Recent evidence indicates that D-serine, rather than glycine itself, is the main and more efficacious endogenous ligand for this glycine site on NMDAR in most brain areas (Mothet *et al.*, 2000). Thus, D-serine and the enzymes involved in its metabolism take part in several physiological and pathological processes related to NMDAR function.

NMDAR-mediated neurotransmission in neonatal rat cerebellar slices is attenuated by D-amino acid oxidase (DAAO), the enzyme that normally degrades D-serine (Mothet *et al.*, 2000). D-amino acid oxidase is also able to reduce granule cell migration (Kim *et al.*, 2005) and to attenuate NMDAR-mediated synaptic transmission in hippocampal slices and cultures, suggesting that endogenous D-serine is essential for maintaining normal synaptic transmission (Mothet *et al.*, 2000). Moreover, endogenous D-serine may set the sensitivity of NMDAR at glutamatergic synapses in the retina (Stevens *et al.*, 2003), regulates the induction of long-term synaptic plasticity in the hippocampus, and contributes to hippocampal cognitive function (Turpin *et al.*, 2011). Furthermore, reduced expression of SR during aging contributes to impairment of hippocampal-dependent cognitive processes (Turpin *et al.*, 2011).

Abnormal NMDAR function has been implicated in the pathophysiology of amyotrophic lateral sclerosis, Alzheimer's disease, and schizophrenia (Labrie & Roder, 2010). A number of susceptibility genes that modulate NMDAR functionality, by encoding for enzymes that regulate the levels of D-serine, are linked to increased risk of schizophrenia (Labrie & Roder, 2010).

D-serine is synthesized from L-serine by SR, a pyridoxal 5'-phosphate-dependent enzyme that catalyzes also the elimination of water from L-serine and D-serine, generating pyruvate and ammonia (De Miranda *et al.*, 2002). D-serine level is also regulated by DAAO, a peroxisomal enzyme whose function is to oxidize D-amino acids to the corresponding imino acids producing ammonia and hydrogen peroxide (Pollegioni & Sacchi, 2010).

Induction of apoptosis involves the activation of genes and protein with pro-apoptotic action and the suppression of genes encoding survival

Correspondence

Nadia Canu, Department of Neuroscience, University of Tor Vergata Via Montpellier 1, 00133 Rome, Italy. Tel.: +39 06 501703233 ext. 3245; fax: +39 06 501703313; e-mail: n.canu@inmm.cnr.it; nadiacanu@tiscali.it

Accepted for publication 24 March 2012

factors. As this may include down-regulation of factors involved in NMDAR function, the aim of this study was to assess the role of SR/D-serine in the apoptosis of rat CGNs. In this report, we identify SR as a crucial player in CGN apoptosis. We show that SR is involved in apoptosis at two phases. First, during the early phase, upstream of caspase activation SR is drastically down-regulated. SR down-regulation is mediated by the ubiquitin proteasome system (UPS) and JNKs. D-serine administration and SR overexpression transiently inhibit apoptosis, whereas pharmacological inhibition of its activity and suppression of its expression exacerbate cell death. In the late phase of apoptosis, the level of SR increases and contributes to the death of last remaining neurons. Taken together, our results suggest that the involvement of SR/D-serine pathway in programmed cell death may contribute to the altered NMDAR activity associated with age- and disease-related brain dysfunction.

Results

Both protein and RNA levels of SR are reduced during CGN apoptosis

Although SR and D-serine were initially detected exclusively in astrocytes ensheathing synapses, a recent report suggests that they are also expressed in neurons both *in vivo* and *in vitro* (Kartvelishvili *et al.*, 2006). Consistent with this finding, we found that primary cultures of CGNs express SR and D-serine (Fig. S1A,B). SR was distributed through the cytosol as well as along neurites, colocalized with GM130 (a Golgi matrix protein) and with Golga-3 (a member of Golgin subfamily) (Figs S1A and 1C). Golga-3 is a SR-binding partner implicated in the regulation of D-serine levels by UPS-mediated degradation of SR (Dumin *et al.*, 2006).

To determine whether KCl withdrawal modulated SR protein level, CGNs grown in a medium containing serum and 25 mM KCl (S+K25) was switched to serum-free medium containing 25 (S-K25) or 5 mM (S-K5) KCl for 1, 3, 6, 12, 24, and 48 h and then processed for Western blotting. The expression profile of SR exhibited a biphasic pattern: the amount of SR protein content progressively declined in the first 24 h (reduction to ~50, 47, and 70% of control value at 6, 12, and 24 h of apoptosis, respectively) and then increased at 48 h, reaching a value which was twice that at 24 h (Fig. 1A,B). Confocal microscope analysis, according to Western blot analysis, showed a marked decrease in SR immunostaining (Fig. 1C). It is worth noting that SR expression in glial cells, which account for only 1% of total cells present in culture, was not affected by KCl deprivation (Fig S2A,B). Analysis of SR mRNA by RT-PCR showed that SR mRNA is substantially reduced within 6 h after the switch to S-K5 (decrease of ~20 and 40% at 3 and 6 h respectively). The same magnitude of decrease was observed both at 12, 24 and to 48 h of apoptosis (Fig. 1D). These findings suggest that different mechanisms regulate levels of SR during early and late phase of apoptosis.

SR down-regulation is regulated by proteasome and JNKs

To identify the key signaling pathways responsible for SR down-regulation during the early phase of CGN apoptosis, we used known anti-apoptotic reagents effective in this paradigm of neuronal death, mainly working upstream caspase activation (Canu *et al.*, 2000, 2005; Butts *et al.*, 2005). The loss of SR protein was counteracted by MG132 (10 μ M), an inhibitor of UPS, and by D-JNKI-1 (1–2 μ M), an inhibitor of JNKs (Borsello *et al.*, 2003) (Fig. 2A,B). D-JNKI-1 also inhibited c-Jun phosphorylation, caspase-3 activation as well as cell death (Fig. S3). By contrast, 3-MA, an inhibitor of autophagy, zVAD-fmk, a pan-caspase inhibitor,

and CAO74-Me, an inhibitor of cathepsin B, were ineffective in counteracting the SR decrease, although they blocked caspase-3 activation and transiently prevented cell death (Canu *et al.*, 2005).

As UPS and JNKs are implicated in the regulation of gene expression and mRNA surveillance and turnover, we tested the effect of UPS and JNK inhibition on apoptosis-induced decrease of SR mRNA. Treatment of CGNs with MG132 and D-JNKI-1 inhibited SR mRNA reduction by ~90 and 15%, respectively (Fig. 2C), suggesting that both UPS and JNKs regulate the levels of SR mRNA.

D-serine is reduced in CGNs undergoing apoptosis

To determine whether reduction in SR was accompanied by reduction in neuronal D-serine content, two methods were applied. In the first, the amount of intracellular D-serine was assayed by immunofluorescence analysis. We found that apoptosis caused a widespread reduction in D-serine immunoreactivity especially prominent in neurons with condensed nuclei (Fig. 3A). In parallel, the amount of D-serine was determined by enzyme-linked immunosorbent assay (ELISA) (Sikka *et al.*, 2010). A representative ELISA standard curve using D-serine-BSA conjugate is shown in Fig. 3B; the detection limit was 0.01 nmoles mg⁻¹. The specificity of the D-serine assay was validated by testing two other amino acids: D-proline and glycine. We found that intracellular D-serine content was reduced by ~15, 30, and 50% at 3, 6, and 12 h of apoptosis, respectively, compared with control (Fig. 3C).

D-serine as a neuroprotectant against apoptosis

To test the contribution of SR activity to apoptosis, we treated CGNs undergoing apoptosis with D-serine or L-serine as control. The culture medium employed did not contain any D-serine, L-serine, or glycine. A loss of ~50% of the neurons was observed within 24 h in S-K5 condition, and addition of D-serine significantly decreased the extent of cell death. MTT assay, intact nuclei count, and morphological examination of cells by phase contrast microscopy showed that, at a concentration of 50 and 100 μ M, D-serine reduced cell death by 45 and 55%, respectively [survival in S-K5 plus D-serine 100 μ M (84 \pm 4%) compared with the same cultures maintained in S-K5 without D-serine (62 \pm 4.52% n = 3, * P < 0.05)] (Fig. 4A,B). At higher concentration (1, 2 mM), the ability to promote neuronal survival was abolished. Neuroprotection by D-serine was blocked by the NMDAR glycine site antagonist 5,7-DCKA (50 μ M), suggesting that D-serine was acting through NMDAR (Fig. 4C). By contrast, L-serine prevented cell death only at high concentration (1–2 mM) (survival of 88 \pm 4% and 76 \pm 3.6 with 2 and 1 mM concentration, respectively; n = 3, ** P < 0.005). However, in this case, protection was not prevented by 5,7-DCKA, indicating that it was not mediated by NMDAR (not shown). Other amino acids (L-threonine and L-leucine) at the same concentrations were not protective (not shown).

D-serine potentiates the neuroprotective action of NMDA against apoptosis

NMDA at a concentration of 100 μ M prevents cell death by blocking the intrinsic pathway of caspase activation (Zhang *et al.*, 1998; Xifro *et al.*, 2005). We found that NMDA (100 μ M) and also D-serine (100 μ M) were able to inhibit SR down-regulation by ~90 and 70%, respectively (Fig. 2B). Then, we evaluated whether the addition of D-serine to neurons induced to undergo apoptosis might modulate or enhance the neuroprotective action of NMDA. Indeed, we found that D-serine was neuroprotective. While NMDA (100 μ M) alone protected 75 \pm 4% of neurons

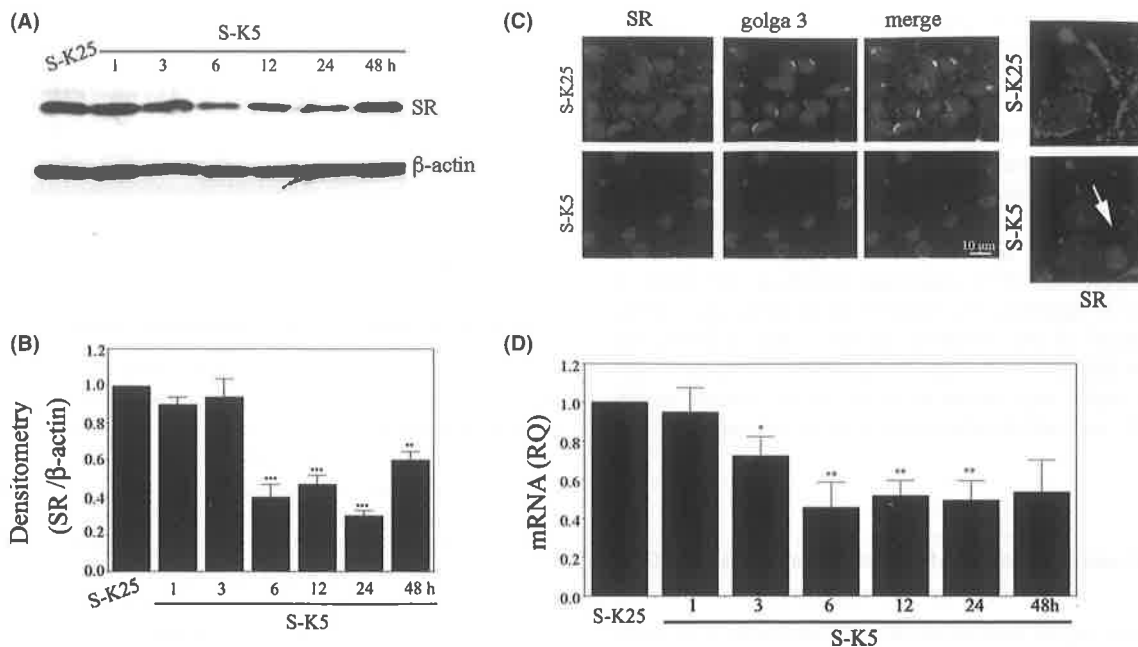


Fig. 1 Expression of SR in cerebellar granule neurons (CGNs) undergoing apoptosis (A) At six DIV, GCNs were washed and maintained in S-K25 for 24 h or switched to S-K5 for the time indicated. Whole cell lysates were analyzed by Western blot with mab anti-SR and β -actin for normalization. (B) Bar graphs depicting quantification of SR immunoreactivity normalized to β -actin protein levels indicate reduction in SR protein level with time. Results were obtained from three separate experiments. $***P < 0.001$, $**P < 0.01$, and one-way ANOVA with Bonferroni's multiple comparison test. (C) Expression of SR (red) and Golgi-3 (green) was assessed by confocal microscopy 6 h after apoptosis induction. Nuclei were stained with Hoechst. To the right of panel B, a higher magnification images for SR expression in S-K5 is reported. Arrow indicates an apoptotic nucleus. (D) Quantitative RT-PCR analysis of SR mRNA levels in CGNs undergoing apoptosis for the time indicated. The amount of SR mRNA was normalized to *TBP* housekeeping gene. Data are reported as mRNA quantification relative to S-K25 control cells [Relative Quantification (RQ)]. Bars represent SD, $*P < 0.05$; $**P < 0.01$.

from cell death, the combined treatment NMDA plus D-serine (100 μ M) had beneficial additive effect saving $95 \pm 3.5\%$ neurons from death [$*P < 0.05$ compared with S-K5+ NMDA (100 μ M)]. Interestingly, it was possible to lowering the concentration of NMDA/D-serine (to 25 μ M each) and retain the same protective effect (Fig. 4D). We proved that the protective action of NMDA/D-serine was accompanied by $\sim 30\%$ inhibition of caspase-3 activation (Fig. 4E).

SR overexpression protects CGNs from apoptosis

We examined whether overexpression of SR could be neuroprotective. At four DIV, CGNs were transduced with adenoviral vectors expressing SR (Ad-SR) and Lac-Z (Ad-Lac-Z) as control. An increase in SR expression was observed with increasing multiplicities of infection (MOI) 48 h post-transduction (Fig. 5A). Confocal analysis showed that SR immunoreactivity was more robust in neurons transduced with Ad-SR (100 MOI) than in control Lac-Z-transduced neurons. Following transduction with Ad-SR and Ad-Lac-Z (100 MOI), we evaluated CGN survival 12 and 24 h after apoptosis induction. Overexpression of SR significantly prevented apoptosis, producing $\sim 90\%$ inhibition of neuronal death at 12 h as compared to control cells transduced with Lac-Z ($**P < 0.01$ compared with Ad-Lac-Z S-K5) (Fig. 5B, see apoptotic nuclei count below Fig. 5E). However, the neuroprotective effect did not extend up to 24 h after the induction of apoptosis, unless L-serine was added to culture medium at the time of apoptosis induction (not shown). Infact, neurons require exogenous L-serine or astrocytes in the culture for D-serine synthesis (Kartvelishvili *et al.*, 2006).

The protective effect exerted by SR overexpression was inhibited by 5,7-DCKA, suggesting that it was mediated by NMDAR (Fig. 5C).

Moreover, we found that in Ad-SR-transduced neurons caspase-3 was less activated (Fig. 5D). This finding was also supported by the lack of caspase-3-mediated truncation of tau protein at the caspase cleavage site D421 (Gamblin *et al.*, 2003) (Fig. 5E).

Potassium-serum deprivation is characterized by changes in several signal transduction pathways including dephosphorylation of Akt-PI3 kinase, ERK-MAPK, and activation of JNKs (D'Mello, 1998). Among these changes, we found that phosphorylation of Akt, in neurons overexpressing SR and induced to undergo apoptosis, was maintained at high levels. In contrast, in apoptotic control neurons, Akt was rapidly dephosphorylated. In addition, we found that SR overexpression prevented Erk 1-2 dephosphorylation until 12 h of apoptosis (Figs 5F,G and 5A), but produced little effects on the increased JNK phosphorylation (Fig. 5F,G).

Pharmacological inhibition of SR and its down-regulation by Sh-RNA increased apoptosis

To determine whether down-regulation of endogenous SR following S-K5 treatment was causally involved in promoting neuronal death, we tested whether pharmacological inhibition or gene silencing of SR would render CGNs more vulnerable to apoptosis. Pharmacological inhibition of SR was evaluated by studying the effect of phenazine metosulphate (Met-Phen), an inhibitor of SR, in cultured CGNs induced to apoptosis. Two different concentrations of this drug (1 and 2 μ M), which inhibited SR activity by $\sim 50\%$ (intracellular D-serine concentration: 6.8 ± 0.77 nmol mg^{-1} protein and 14 ± 1.3 nmol mg^{-1} protein in S-K25 plus or without Met-Phen, respectively; $n = 3$, $**P < 0.005$) without toxicity as previously reported (Kim *et al.*, 2005; Sasabe *et al.*, 2007), were administered at the time of apoptosis induction. We found that Met-Phen

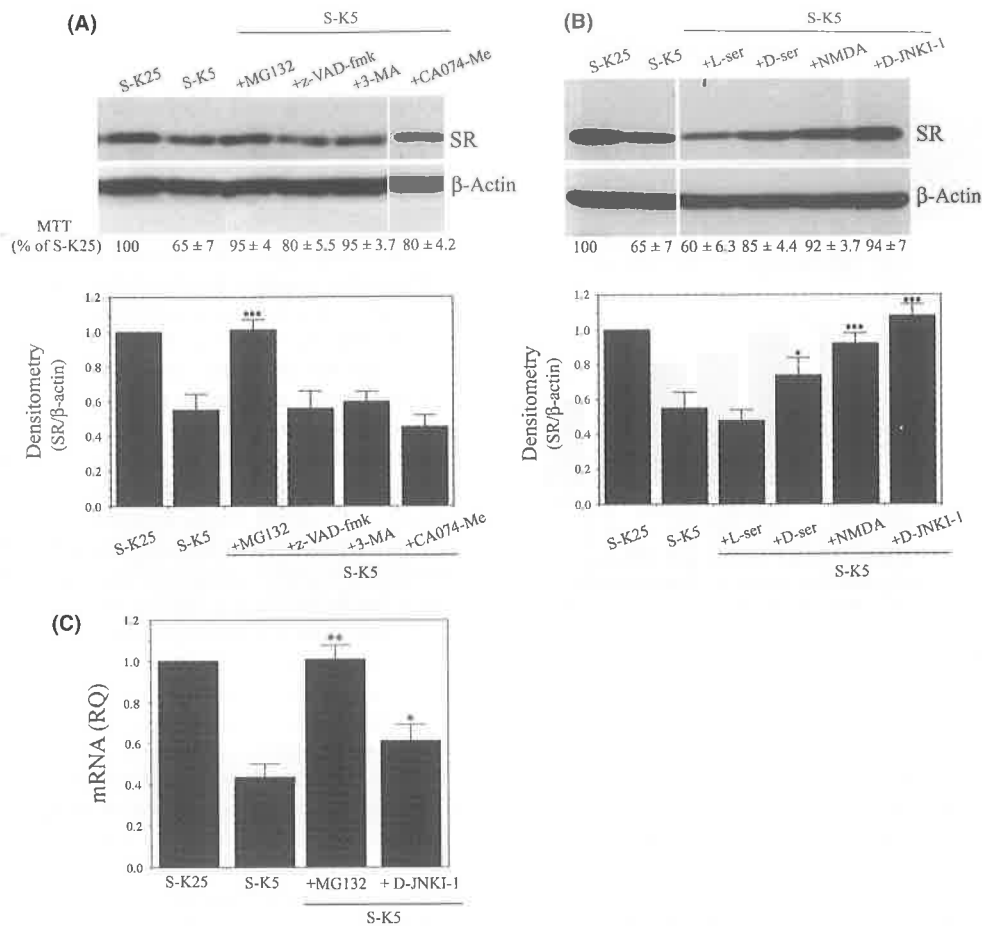


Fig. 2 Effect of various anti-apoptotic factors on SR down-regulation (A) and (B) cerebellar granule neurons (CGNs) were induced to undergo apoptosis in the absence or in the presence MG132 (10 μ M), zVAD-fmk (100 μ M), 3-MA (10 mM), and CA074-Me (100 μ M) or in the presence of L-serine (100 μ M), D-serine (100 μ M), NMDA (100 μ M), or D-JNK1-1 (2 μ M) for 12 h. Western blot and quantification of SR immunoreactivity were performed as reported in Fig. 1. For each experimental condition, the corresponding MTT assay is reported below Western blot. (C) Quantitative RT-PCR analysis of SR mRNA levels in CGNs undergoing apoptosis in the absence or in the presence of MG132 and D-JNK1.1. In this case, the amount of SR mRNA was normalized to β -actin housekeeping gene because TBP housekeeping gene is modulated by D-JNK1.1. Data are reported as in Fig. 1C. Bars represent SD, * P < 0.05; ** P < 0.01.

dramatically increased neuronal death as provided by MTT bioreduction and nuclei count, over a 24-h period (Fig. 6A). No effect on neuronal survival in S-K25 was observed.

We also examined the effect of SR silencing during apoptosis. Cerebellar granule neurons were infected at two to three DIV with lentiviral particles for Sh-RNA/SR and Sh-RNA/scramble as control. Western blot analysis performed on neuronal lysates 72 h after infection, indicated that the Sh-RNA/SR reduced SR expression by \sim 70%. By contrast, SR expression in control neurons infected with Sh-RNA/scramble was unaffected. Moreover, β -actin in Sh-RNA/SR neurons did not show significant changes in expression compared with Sh-RNA/scramble neurons, indicating effectiveness and specificity of the silencing (Fig. 6B). In addition to increasing cell death (Fig. 6C), SR silencing increased dephosphorylation of Akt (Fig. 6B), activation of caspase-3, and decreased phosphorylation of JNKs (Fig. 6B).

Increased SR levels characterize the late stage of apoptosis

As shown in Fig. 1A, 48 h after apoptosis induction, the protein amount of SR reached a value, which was twice that at 24 h of apoptosis. This trend was also confirmed by confocal microscope analysis of SR immuno-

staining. Indeed, apoptotic neurons with highly condensed nuclei surrounded by a small rim of cytoplasm were strongly immunoreactive for SR (Fig. 6E). As the amount of extracellular D-serine was markedly increased 48 h after apoptosis induction [being $0.5 \pm 0.13 \mu$ M in S-K25 and $10.3 \pm 0.7 \mu$ M in S-K5 ($n = 4$, *** P < 0.001)], we examined whether the SR inhibitor Met-Phen could recover this last population of neurons from cell death. We found that addition of Met-Phen inhibitor (1–2 μ M) 48 h after apoptosis induction increased the number of viable cells from \sim 20 (in the absence of Met-Phen) to \sim 40% (in the presence of Met-Phen) at 72 h of apoptosis (Fig. 6F). Interestingly, the same neuroprotective effect was exerted by MK801 (Fig. 6G), an NMDAR antagonist. All together, these findings suggest that SR is involved in this last, NMDAR-mediated, wave of cell death.

Discussion

Our study provides the first evidence that SR/D-serine pathway plays a role in CGN apoptosis and that signals generated by an apoptotic event influence the expression of factors whose activity is dispensable for full activation of NMDAR. We found that SR protein and mRNA are modulated very early in CGN apoptosis. Interestingly, a biphasic

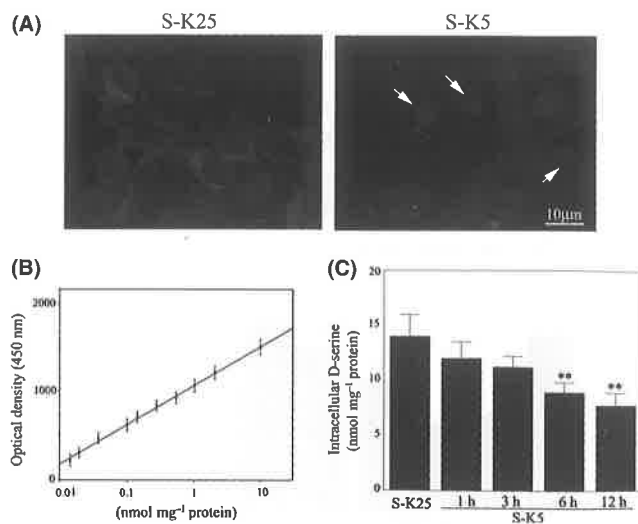


Fig. 3 D-serine content in cerebellar granule neurons (CGNs) undergoing apoptosis. (A) Confocal microscope evidences a marked reduction in SR immunoreactivity (red) in apoptotic neurons (S-K5 for 6 h, blue, arrows). (B) Representative standard curve in the ELISA of D-serine obtained by immobilizing the D-amino acid at concentration indicated onto assay plates. Each data point was averaged (\pm SEM) from three experiments. (C) Bar graph of mean D-serine level (\pm SEM) determined by ELISA in control (S-K25) and CGNs undergoing apoptosis for the time indicated.

expression pattern for SR protein was observed during apoptosis, with a drastically drop of protein level by 50% and 70% at 6 and 24 h after apoptosis induction, respectively, and a second wave of expression in the late phase of apoptosis. In the first phase of apoptosis, the SR protein decline may be due to reduced SR transcription. This suggestion is based upon the effects of UPS and JNKs inhibition on SR mRNA levels during apoptosis (Fig. 2). UPS and JNKs are two fundamental players in CGN apoptosis (Canu *et al.*, 2000; Harris *et al.*, 2002), and they likely converge on c-Jun for regulating SR expression during apoptosis. Indeed, c-Jun, whose expression and phosphorylation increase rapidly after KCl withdrawal (D'Mello, 1998; Xifro *et al.*, 2005), is known to increase SR mRNA level through a JNK-dependent recruitment of AP-1 complex consisting of a Fos and Jun, on SR promoter (Wu & Barger, 2004). However, in our experimental conditions, JNK/Jun should reduce SR transcription. Difference between the two scenarios may be, in part, due to the composition of AP-1 complex. c-Jun-mediated CGN apoptosis requires the activation of transcription factor-2 (ATF2) and the concomitant down-regulation of c-Fos (Yuan *et al.*, 2009). Thus, different AP1 complex might differentially affect transcription of SR gene. However, posttranscriptional (e.g. mRNA stability) and posttranslational mechanisms may also contribute to modulate SR expression. As SR has a relatively short half-life, and its turnover is regulated by UPS (Dumin *et al.*, 2006), it is reasonable to suppose that, in the early stages of apoptosis, the activation of UPS (Canu *et al.*, 2000) might degrade SR. Nuclear run-on transcription assay and pulse-chase experiments will further clarify the mechanisms underlying these observations.

As a reduction in intracellular D-serine level accompanies depletion of SR, we evaluated the effects of D-serine addition on survival. D-serine, at concentration of 50–100 μ M, was able to recover ~20–25% of neurons from cell death through an NMDAR-dependent mechanism. This suggests that added D-serine in conjunction with glutamate, spontaneously released from vesicles in S-K5 (Mellor *et al.*, 1998), is able to activate NMDAR. The finding that glycine (100 μ M) has no detectable effect on

apoptosis and on survival promoting activity of NMDA (Bhave & Hoffman, 1997) suggests that NMDAR complex is more sensitive to D-serine than to glycine.

At higher concentration, D-serine did not produce notable effects. A likely explanation for this observation may involve $\alpha\beta$ -elimination activity of SR. This activity, documented in cortical neurons cultivated in presence on 2 mM of D-serine, converts D-serine to pyruvate and ammonia and is believed to monitor D-serine level (Foltyn *et al.*, 2005). However, preliminary observations indicate that pyruvate concentration is not increased in apoptotic neurons in the presence of 2 mM of D-serine (not shown), suggesting that $\alpha\beta$ -elimination activity is not implicated. A more plausible alternative hypothesis should involve D-serine uptake, likely through low-affinity Na⁺-dependent D-serine uptake (Shao *et al.*, 2009) and D-serine degradation by DAAO. The last is a flavoenzyme that metabolizes certain D-amino acids (D-alanine, D-proline, and D-leucine and D-serine). By microarray assay, we found that the DAAO gene is significantly up-regulated (fold change: 2.01, $P = 0.0245$) in CGN apoptosis and that its activity is increased by +82%, +170%, and +90% at 1, 3, and 6 h of apoptosis, respectively ($P < 0.05$) as compared to control non apoptotic neurons (Fig. S5A,B). Although, DAAO is conventionally described as being a glial enzyme particularly enriched in cerebellum, there is increasing evidence of its presence also in neuronal cells (Verrall *et al.*, 2010). Moreover, DAAO and SR, when present in the same cells, do not work in isolation; for example, their activities are regulated in opposite way by nitric oxide to tightly regulate D-serine level (Shoji *et al.*, 2006).

Although the protective effects observed in the presence of 1 and 2 mM of L-serine could be related to NMDAR activation after conversion of L-serine to D-serine in neurons, the inability of 5,7-DCKA to counteract this effect does not favor this hypothesis. It is likely that L-serine might be converted into phosphatidylserine or cystathionine, which signals cell survival (Kartvelishvili *et al.*, 2006; Tay *et al.*, 2010).

Further support for the involvement of SR on CGN survival was obtained by overexpressing and down-regulating SR. In the first case, we detected protection against cell death, exerted through preservation of high levels of P-Akt and inhibition of caspase-3 activation in manner comparable to NMDA-mediated neuroprotection. In the second case, increased cell death was accompanied by increased dephosphorylation of Akt and caspase activation. Although our findings indicated an NMDAR-mediated involvement of SR in CGN apoptosis, we cannot exclude other mechanisms. It is possible that SR down-regulation may render Golgi-3, a substrate of caspase-3 leading to its cleavage and contributing to Golgi dispersal. As to the increased SR expression in the late stage of apoptosis (Figs 1A and 6E,F), we found that it is not because of an increase in SR mRNA levels (Fig. 1D). We therefore hypothesize that it may be due to caspase-3-mediated decay of UPS activity (Canu *et al.*, 2000) and golgin cleavage. Although the resulting SR accumulation might be the last effort to save neurons, actually it is responsible for the death of neurons in the late stages of apoptosis. This statement, raised from finding that Met-Phen and MK801 blocked this second wave of cell death, allows to speculate that SR [likely derived from phospholipids or from glycine (Kartvelishvili *et al.*, 2006) or from protein degradation] could be, through the conversion of L-serine into D-serine and thus the activation of NMDAR, one of the players involved in the transition from apoptosis to necrosis, described in this model of programmed cell death *in vitro* (Villalba *et al.*, 1997).

In conclusion, our results show that the deregulation of SR/D-serine pathway may interfere with the NMDAR-mediated promotion of neuronal health. This may be relevant to those pathophysiological conditions characterized by a coexistence of apoptosis and NMDAR dysfunction.

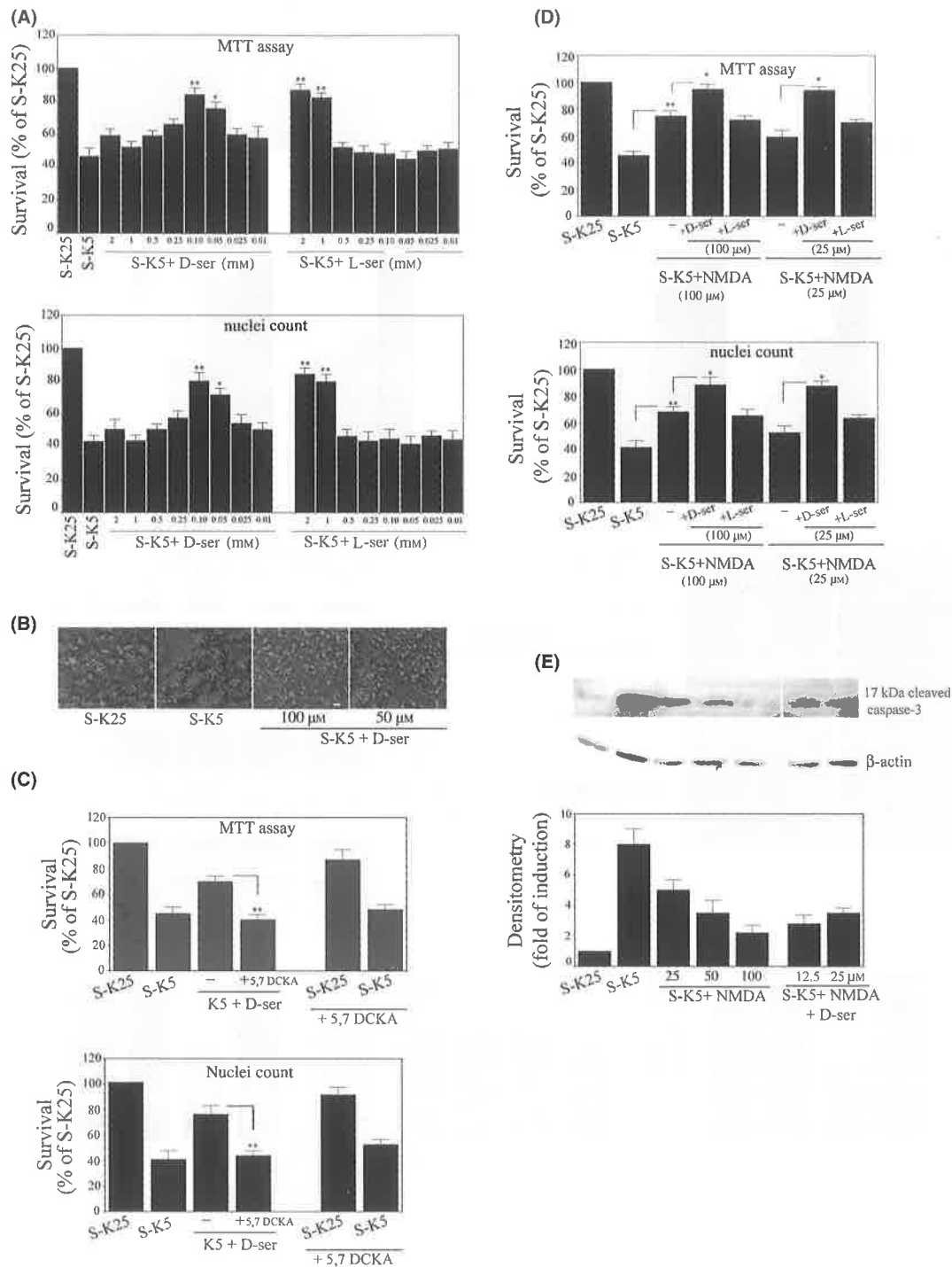


Fig. 4 D-serine blocks apoptosis and potentiates the neuroprotective action of NMDA (A). Apoptosis was induced in the absence or in the presence of different concentrations D-serine and L-serine. After 24 h, cell viability was determined as indicated. Results are the means \pm SEM of duplicate determinations from three independent experiments and are reported as percentage of control cells (S-K25 for 24 h), $**P < 0.01$ compared with S-K5. (B) Micrographs of cultures upon 24 h of apoptosis in the absence or presence of 100 and 50 μM of D-serine. Phase contrast images have been inverted using the regulation tool of Adobe Photoshop. (C) Apoptosis was induced in the absence or presence of D-serine (50 μM) and 5,7 DCKA (50 μM) for 24 h. Viability was determined as indicated and data reported as in A. It should be noted that 5,7 DCKA treatment did not affect survival neither in S-K25 nor in S-K5 cells, $**P < 0.01$ compared with S-K5 + D-serine. (D) Survival of cerebellar granule neurons (CGNs) assayed at 24 h of apoptosis in the absence or presence NMDA (100 and 25 μM), and in the absence or presence of D-Ser or L-Ser (100 and 25 μM) plus NMDA (100 and 25 μM). Data are reported as in A, $**P < 0.01$ compared with S-K5; $*P < 0.05$ compared with S-K5 + NMDA (100 μM) and S-K5 + NMDA (25 μM). (E) Representative Western blot analysis for cleaved caspase-3 and its densitometric evaluation, normalized to β -actin, in CGNs undergoing apoptosis for 12 h in the absence or presence of NMDA (25, 50, and 100 μM) or in the presence of D-serine plus NMDA (12.5 and 25 μM each). Data, reported as fold of induction of the amount cleaved caspase-3 in control S-K25 cells, which have been given a value of 1, are the mean (\pm SEM) of three independent experiments.

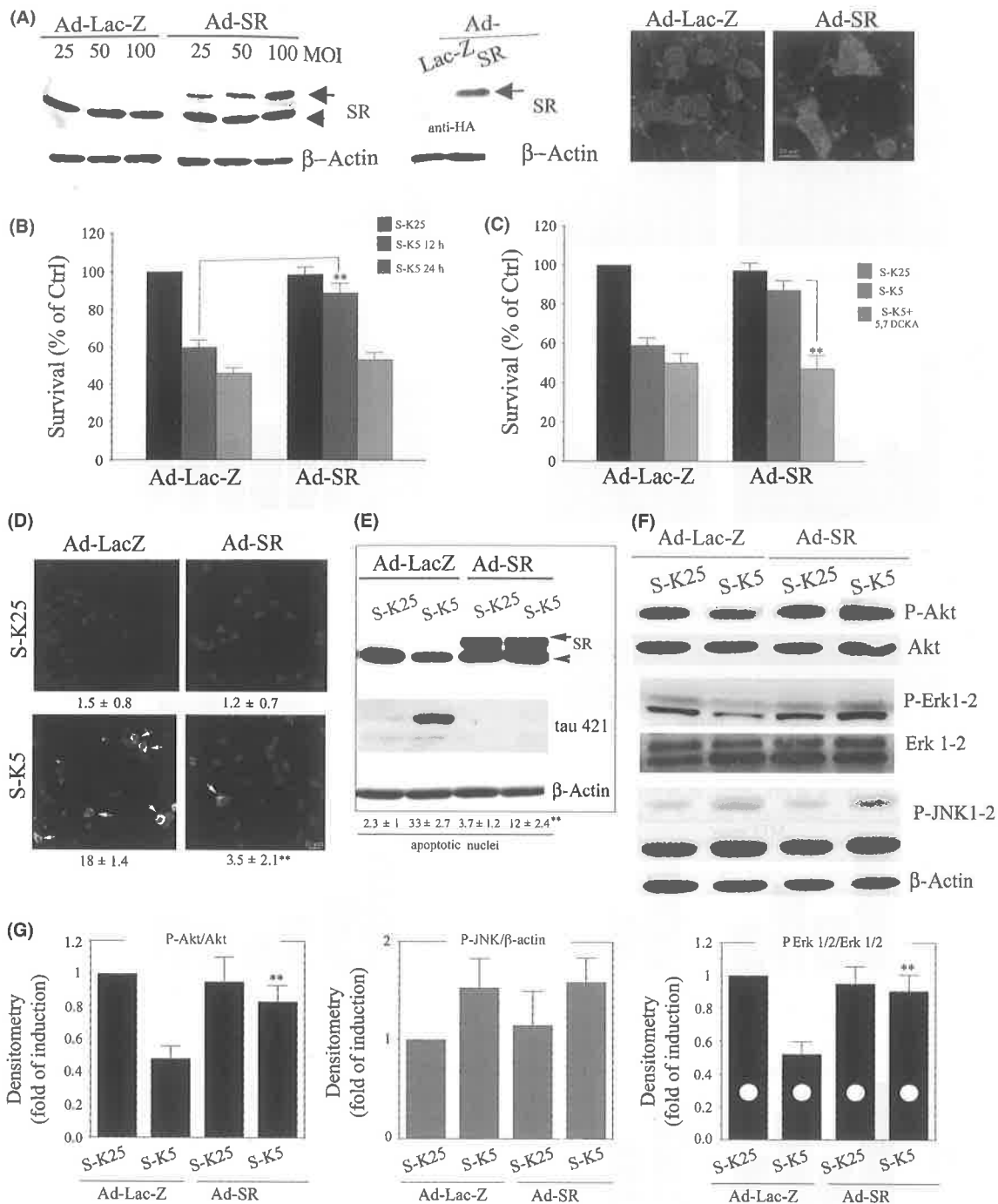


Fig. 5 Protection mediated by SR overexpression involves inhibition of caspase-3 activation, tau cleavage, and P-Akt dephosphorylation. Cerebellar granule neurons (CGNs) were transfected at four DIV with either Lac-Z- or SR-expressing adenovirus particles at the MOIs indicated. At six DIV, lysates were subjected to Western blot analysis, with anti-SR, anti-HA, and β -actin for normalization, and to immunofluorescence analysis with goat anti-SR. Arrow and arrowhead indicate exogenous and endogenous SR, respectively. (B) Survival was assessed 12 and 24 h later by MTT assay. Each data point is the mean \pm SEM of triplicate determinations of three independent experiments and is expressed as percentage of S-K25 Ad-Lac-Z cells (100%), $***P < 0.01$ compared with Ad-Lac-Z neurons. (C, D) Survival of transfected neurons undergoing apoptosis for 12 h in the absence or in the presence of DCKA. Data are reported as in A. (E) Immunostaining for cleaved caspase-3 (Asp 175) (green) and counterstaining with Hoechst for nuclei (blue) 8 h after apoptosis induction. Notice that SR overexpression reduces the number of cleaved caspase-3-positive neurons (arrows). Values corresponding to the number of cleaved caspase-3-positive neurons as percentage of total cells (\pm SEM) are reported below, $***P < 0.01$ compared with Ad-Lac-Z in S-K5. (F) Tau cleavage was analyzed 12 h after induction of apoptosis by immunoblotting with mAb Tau421 antibody [tau-C3] and β -actin as efficiency of transduction and loading control. Values corresponding to the number of apoptotic nuclei as percentage of total nuclei (\pm SEM) are reported below, $***P < 0.01$ compared with Ad-Lac-Z in S-K5. (F) Lysates from Ad-Lac-Z- and Ad-SR-transfected CGNs undergoing apoptosis for 3 h were probed for phospho Akt (P-Akt), total Akt, phospho Erk 1-2 (P-Erk1-2), total Erk 1-2, phospho JNK (P-JNK), and β -actin for loading control. (G) Bar graphs depict quantification of immunoreactivity for P-Akt, normalized to total Akt, for P-JNK normalized to β -actin protein, and P-Erk1-2 normalized to total Erk 1-2 levels. Results were obtained from three separate experiments: $***P < 0.001$, $**P < 0.01$, one-way ANOVA with Bonferroni's multiple comparison test.

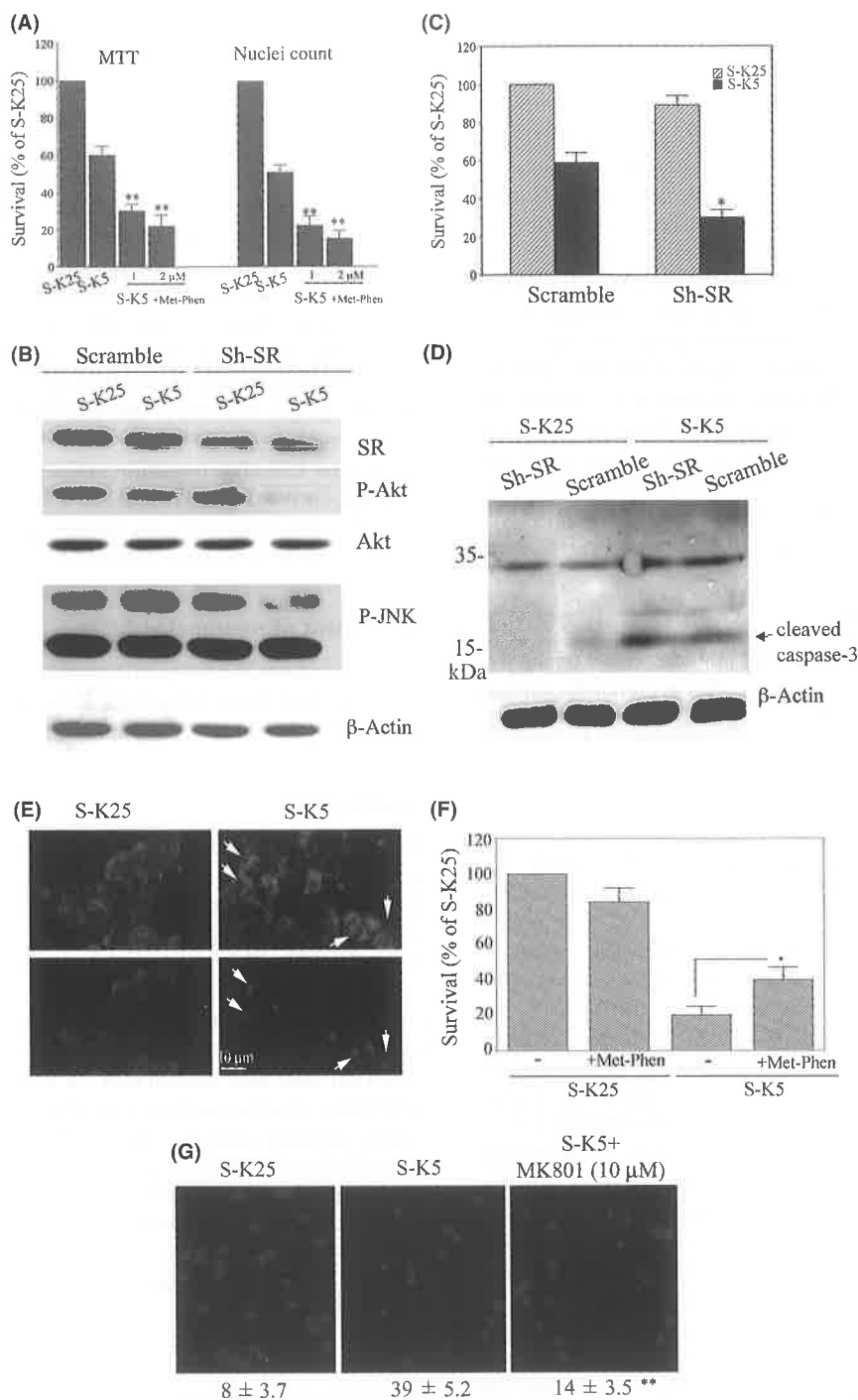


Fig. 6 Inhibition of SR activity and down-regulation of its expression exacerbate cell death (A), CGNs were exposed to 1–2 μM Met-Phen either 1 h before or at the time of apoptotic stimulus. The number of viable cells, determined 24 h later, is reported as mean ± SEM of triplicate determinations of three independent experiments and expressed as percentage of S-K25 Ad-Lac-Z cells (100%), ** $P < 0.01$ compared with Ad-Lac-Z neurons in S-K5. (B) CGNs (one DIV) were transfected either with scramble or with Sh-SR lentivirus. At six DIV, they were induced to undergo apoptosis for 3 h when lysates were processed for immunodetection of SR, P-Akt, Akt, P-Erk 1-2, P-JNK, and β-actin as control of silencing efficiency and loading. (C) Survival of CGNs, transfected as reported in (B), was assessed 24 h after apoptosis induction, by MTT assay. Each data point is the mean ± SEM of triplicate determinations of three independent experiments and is expressed as percentage of S-K25 scramble neurons (100%), ** $P < 0.01$ compared with Ad-Lac-Z neurons. (D) A representative Western blot showing level of 17-kDa proteolytic fragment of activated caspase-3 (arrow) at 12 h of apoptosis in CGNs infected with scramble and ShSR lentiviruses. Loading control: β-actin. Increased SR levels in the late stage of apoptosis contribute to the last wave of cell death. (E) Confocal microscope analysis showing the increase in SR immunoreactivity in apoptotic neurons (S-K5) recognizable as those having a condensed nuclei strongly stained by Hoechst (blue). (F) Survival of CGNs at 72 h in the absence or in the presence of Met-Phen (1 μM) added to culture medium 48 h after apoptosis induction. Each data point is the mean ± SEM of triplicate determinations of three independent experiments and is expressed as percentage of S-K25 at 72 h. * $P < 0.1$ compared with S-K5 at 72 h. (G) Micrographs of Hoechst 33258-stained cultures upon 72 h of apoptosis in the absence or presence of MK801 added to medium 48 h after apoptosis induction. Values corresponding to the number of condensed nuclei as percentages of total nuclei are reported below. ** $P < 0.01$ compared with S-K5 at 72 h.

Experimental procedures

N-methyl-D-aspartic acid (NMDA), phenazine methosulfate (Met-Phen), D-serine, L-serine, 3MA (3 methyladenine), MG132 (z-Leu-Leu-Leu-al), (+)-MK-801 hydrogen maleate, 5,7-dichlorokynurenic acid (5,7-DCKA), zVAD-fmk, and CA074-Me were from Calbiochem. D-JNK11 was provided by T. Borsello. Goat D-serine racemase antibody was from Santa Cruz Biotechnology, Inc. (Santa Cruz, CA, USA). Mouse D-serine racemase antibody was from BD transduction laboratory. Rabbit D-serine antibody was from GemacBio (Cenon Cedex, France). Rabbit anti-Golga-3 antibody was provided by Dr Matsukuma (Kanagawa Cancer Center Research Institute, Yokohama, Japan). Rabbit anti-GM130 and mouse anti- β -actin-HRP were from Sigma-Aldrich (St. Louis, MO, USA). Rabbit anti-caspase-3 and anti-cleaved caspase-3 (Asp175), Phospho 44/42 MAP kinase, Phospho SAPK/JNK, Phospho Jun, Phospho Akt, AKT, and 44/42 MAP kinase antibodies were from Cell Signaling Technology, Inc. (Danvers, MA, USA). Mouse monoclonal Tau421 antibody [tau-C3] was from Abcam. All HRP and fluorescent-conjugated antibodies were from Jackson ImmunoResearch. The specificity of anti-SR, GM130, and Golga-3 antibodies in CGNs is reported in Fig. S1.

Preparation of CGN cultures

Cerebellar granule neurons were obtained from dissociated cerebella of 8-day-old Wistar rats (Charles River, Calco, Italy) as previously described (Canu *et al.*, 2005), see Data S1, (Supporting information).

Real-Time PCR

Total RNA from CGN was extracted by illustra QuickPrep Micro mRNA Purification Kit (GE Healthcare Europe GmbH, Freiburg, Germany) including a DNase treatment before elution from the column. RNA (0.5 μ g) was reverse transcribed for 50 min at 42 °C in a 40 μ l reaction containing 200 ng of random hexamers (GE Healthcare Europe GmbH), 5 \times first-strand buffer (Invitrogen), 10 mM DTT, 0.25 mM deoxynucleotides (0.25 mM each dATP, dGTP, dCTP, and dTTP; Invitrogen), and 400 units of M-MLV RT (Invitrogen, Carlsbad, CA, USA). Equal amount of cDNA was taken for quantitative RT-PCR carried out using an Applied Biosystem 7900HT Fast RT-PCR System instrument. Each PCR contained sense and antisense primers at a concentration of 200 nM in a final volume of 12 μ l of Sensimix Plus SYBR (Quantance QT605-05). Primers were designed with the assistance of ProbeFinder Software (Roche Applied Science, Indianapolis, IN, USA) and spanned an intron-exon junction. The following primers were used: rat SR (GenBank (NM_198757) 5'- gct gtg aga agg aag cca ac (fwd) and 5'- ctg agc aca cat ggt ttt gaa (rev); rat TBP: 5'-ccc acc agc agt tca gta gc-3' (fwd) and 5'-caa ttc tgg gtt tga tca ttc tg-3' (rev); and rat β -actin: 5'-caa ctg gga cga tat gga gaa g-3' (fwd) and 5'-tct cct tct gca tcc tgt cag-3' (rev). Specificity was confirmed by dissociation curve and agarose gel analysis. The PCR conditions were as follows: 95 °C for 10 min, followed by 40 cycles of 95 °C for 15 s and 60 °C for 1 min.

Construction and purification of recombinant adenovirus

Full-length mouse SR cDNA was generated by PCR amplifications using vector as template (provided by Dr. Wolosker). PCR primers contained Nhe I (5') and Not I (3') sequences for insertion into NheI-Not I sites of pShuttle vector (Clontech). Replication-deficient Ad5 adenoviral vector-encoding mouse HA-SR was prepared,

amplified, purified, and transduced as previously reported (Amadoro *et al.*, 2004).

Sh-RNA-mediated suppression by lentivirus

A small hairpin RNAs (Sh-RNAs), the 19-nucleotide GGCGNAAT-CTCTTCTCAA (444-463) of rat SR mRNA (NCBI accession number NM_198757), were designed. The expression cassette containing sense loop (TTCAAGAGA) and antisense termination signalT was cloned into BamHI-EcoRI site of pLV-THM vector, generating the new lentiviral vectors pLV-TH Sh-RNA/SR and pLV-TH Sh-RNA/scramble. Lentiviruses were produced by transient cotransfection in HEK 293T of 20 μ g of a plasmid vector, 15 μ g of pAX2, and 6 μ g of pMD2G-VSVG (Zufferey *et al.*, 1998). After 48 h, the medium was centrifuged at 1000 g for 10 min to remove cellular debris. High-titer stocks were obtained by ultracentrifugation. Viral titers, expressed as the number of transducing units per milliliter (TU mL⁻¹), were determined by counting the number of GFP positive cells after transducing HEK293T cells in limiting dilutions. Viruses at 1×10^6 TU mL⁻¹ were used in the experiments. Transduction was performed at one DIV. Cells remained in contact with the lentivirus for 5 h when the medium was replaced with fresh BME.

Assessment of neuronal viability

Viability was quantified by the MTT tetrazolium salt assay, by counting the number of intact nuclei (Canu *et al.*, 2005), or the number of condensed nuclei after Hoechst 33342 staining.

D-serine assay

The D-serine enzyme-linked immunosorbent assay (ELISA) was performed according to the study by Sikka *et al.*, 2010, with minor modifications: 25 μ l of glutaraldehyde (0.02 M) was added to 100 μ l of each extract (adjusted to 0.5 mg mL⁻¹ with water) or D-serine standards (0.06–15 nmol mL⁻¹) in PBS containing 0.2 mg mL⁻¹ BSA. Then, 50 μ l triplicate of the mixed solutions was added to an ELISA plate for 2 h at RT. After three washes with PBST [10 mM sodium phosphate, 2 mM potassium phosphate pH 7.4, 140 mM NaCl, 3 mM KCl, and 0.02% (vol/vol) Tween 20], wells were blocked with 2% nonfat milk in PBST for 60 min at RT. Plates were then washed three times in PBST (300 μ l). Rabbit anti-D-serine antibody diluted 1:1500 in PBST containing 1% BSA was pre-incubated for 1 h at RT before being added (50 μ l) to each well. After 1-h incubation, the HRP-linked donkey anti-rabbit 1:1000 antibody was added for 30 min, followed by three washes in PBST. A colorimetric reaction initiated by the addition of 50 μ l TBM to each well was measured at 690 nm after stopping the reaction with 0.2 N HCl.

Western Blot analysis

Total proteins prepared in SDS/reducing sample buffer were subjected to SDS-PAGE and transferred to nitrocellulose paper (Hybond-C, Amersham Biosciences). After incubation for 2 h in blocking buffer (TBS+5% nonfat dry milk), membranes were exposed to primary antibody at 4 °C. Incubation with secondary peroxidase-coupled anti-mouse/anti-rabbit was performed using the ECL system (Amersham Bioscience). Bands of interest were measured using NIH IMAGEJ densitometry software.

Immunofluorescence

Cerebellar granule neurons were cultured in the chamber slides, fixed, and permeabilized with methanol 100% for 20 min at -20 °C. After

blocking with 4% normal goat serum in PBS, the slides were incubated with affinity-purified goat anti-SR (1:50) overnight at 4 °C. Secondary antibody consisted of a TRITC-conjugated anti-goat used at 1 µg mL⁻¹.

Immunofluorescence for intracellular D-serine levels was performed with anti-glutaraldehyde-BSA-conjugated D-serine antibody. Briefly, CGNs were fixed in 4% paraformaldehyde/0.1% glutaraldehyde in PBS. After reduction in free aldehyde group with 0.5% sodium borohydride (three times for 5 min each), CGNs were permeabilized in 0.2% Triton X-100 in PBS, blocked for 45' at RT with 5% donkey serum and incubated at 4 °C overnight with rabbit anti-D-serine (1:1000). Control cells were incubated with antibody pre-absorbed with D-serine-G-BSA (Gemac Bio).

Slides were examined under a confocal laser scanning microscope (Leica SP5; Leica Microsystems, Wetzlar, Germany) equipped with four laser lines: violet diode emitting at 405 nm, argon emitting at 488 nm, helium/neon emitting at 543 nm, and helium/neon emitting at 633 nm. All analyses were performed in sequential scanning mode to rule out cross-bleeding between channels. Images of Fig. S1 were captured on a Leika fluorescence microscope. Final figures were assembled using ADOBE PHOTOSHOP 6.

Statistics

All data were expressed as the means ± SEM for three of four independent experiments. Unless otherwise mentioned, statistical analysis was performed using *t* test (Student's *t* test).

Acknowledgments

This work was supported by grants from PRIN 2009 (2009KP83CR) and from Fondi di Ateneo to NC. We thank P. Calissano and S. Biocca for comments on this manuscript. We are grateful to Dr. Wolosker for providing mouse SR-HA cDNA and Dr. Matsukuma for anti-Golga-3 antibody. The Authors declare that there is no conflict of interest.

References

Amadoro G, Serafino AL, Barbato C, Ciotti MT, Sacco A, Calissano P, Canu N (2004) Role of N-terminal tau domain integrity on the survival of cerebellar granule neurons. *Cell Death Differ.* **11**, 217–230.

Bhave SV, Hoffman PL (1997) Ethanol promotes apoptosis in cerebellar granule cells by inhibiting the trophic effect of NMDA. *J. Neurochem.* **68**, 578–586.

Borsello T, Clarke PG, Hirt L, Vercelli A, Repici M, Schorderet DF, Bogouslavsky J, Bonny C (2003) A peptide inhibitor of c-Jun N-terminal kinase protects against excitotoxicity and cerebral ischemia. *Nat. Med.* **9**, 1180–1186.

Burgoyne RD, Cambray-Deakin MA (1988) The cellular neurobiology of neuronal development: the cerebellar granule cell. *Brain Res.* **472**, 77–101.

Butts BD, Hudson HR, Linseman DA, Le SS, Ryan KR, Bouchard RJ, Heidenreich KA (2005) Proteasome inhibition elicits a biphasic effect on neuronal apoptosis via differential regulation of pro-survival and pro-apoptotic transcription factors. *Mol. Cell. Neurosci.* **30**, 279–289.

Canu N, Barbato C, Ciotti MT, Serafino A, Dus L, Calissano P (2000) Proteasome involvement and accumulation of ubiquitinated proteins in cerebellar granule neurons undergoing apoptosis. *J. Neurosci.* **20**, 589–599.

Canu N, Tufi R, Serafino AL, Amadoro G, Ciotti MT, Calissano P (2005) Role of the autophagic-lysosomal system on low potassium-induced apoptosis in cultured cerebellar granule cells. *J. Neurochem.* **92**, 1228–1242.

De Miranda J, Panizzutti R, Foltyn VN, Wolosker H (2002) Cofactors of serine racemase that physiologically stimulate the synthesis of the N-methyl-D-aspartate (NMDA) receptor coagonist D-serine. *PNAS* **99**, 14542–14547.

D'Mello SR (1998) Molecular regulation of neuronal apoptosis. *Curr. Top. Dev. Biol.* **39**, 187–213.

D'Mello SR, Galli C, Ciotti T, Calissano P (1993) Induction of apoptosis in cerebellar granule neurons by low potassium: inhibition of death by insulin-like growth factor I and cAMP. *PNAS* **90**, 10989–10993.

Dumin E, Bendikov I, Foltyn VN, Misumi Y, Ikehara Y, Kartvelishvily E, Wolosker H (2006) Modulation of D-serine levels via ubiquitin-dependent proteasomal degradation of serine racemase. *J. Biol. Chem.* **281**, 20291–20302.

Foltyn VN, Bendikov I, De Miranda J, Panizzutti R, Dumin E, Shleper M, Li P, Toney MD, Kartvelishvily E, Wolosker H (2005) Serine racemase modulates intracellular D-serine levels through an alpha, beta-elimination activity. *J. Biol. Chem.* **280**, 1754–1763.

Gallo V, Kingsbury A, Balázs R, Jørgensen OS (1987) The role of depolarization in the survival and differentiation of cerebellar granule cells in culture. *J. Neurosci.* **7**, 2203–2213.

Gamblin TC, Chen F, Abraha A, Miller R, Fu Y, Garcia-Sierra F, Lagalwar S, Berry RW, Binder LI, Cryns VL (2003) Caspase cleavage of tau: linking amyloid and neurofibrillary tangles in Alzheimer's disease. *PNAS* **100**, 10032–10037.

Hardingham GE (2006) Pro-survival signalling from the NMDAR. *Biochem. Soc. Trans.* **34**, part 5, 936–938.

Harris C, Maroney AC, Johnson EM Jr (2002) Identification of JNK dependent and independent components of cerebellar granule neuron apoptosis. *J. Neurochem.* **83**, 992–1001.

Hetman M, Kharebava G (2006) Survival signaling pathways activated by NMDARs. *Curr. Top. Med. Chem.* **6**, 787–799.

Johnson JW, Ascher P (1990) Voltage-dependent block by intracellular Mg²⁺ of N-methyl-D-aspartate-activated channels. *Biophys. J.* **57**, 1085–1090.

Kartvelishvily E, Shleper M, Balan L, Dumin E, Wolosker H (2006) Neuron-derived D-serine release provides a novel means to activate N-methyl-D-aspartate receptors. *J. Biol. Chem.* **281**, 14151–14162.

Kim PM, Aizawa H, Kim PS, Huang AS, Wickramasinghe SR, Kashani AH, Barrow RK, Haganir RL, Ghosh A, Snyder SH (2005) Serine racemase: activation by glutamate neurotransmission via glutamate receptor interacting protein and mediation of neuronal migration. *PNAS* **102**, 2105–2110.

Labrie V, Roder JC (2010) The involvement of the NMDA receptor D-serine/glycine site in the pathophysiology and treatment of schizophrenia. *Neurosci. Biobehav. Rev.* **34**, 351–372.

Mellor JR, Merlo D, Jones A, Wisden W, Randall AD (1998) Mouse cerebellar granule cell differentiation: electrical activity regulates the GABA receptor alpha 6 subunit gene. *J. Neurosci.* **18**, 2822–2833.

Monti B, Contestabile A (2000) Blockade of the NMDA receptor increases developmental apoptotic elimination of granule neurons and activates caspases in the rat cerebellum. *Eur. J. Neurosci.* **12**, 3117–3123.

Mothet JP, Parent AT, Wolosker H, Brady RO Jr, Linden DJ, Ferris CD, Rogawski MA, Snyder SH (2000) D-serine is an endogenous ligand for the glycine site of the N-methyl-D-aspartate receptor. *PNAS* **297**, 4926–4931.

Nardi N, Avidan G, Daily D, Zilkha-Falb R, Barzilai A (1997) Biochemical and temporal analysis of events associated with apoptosis induced by lowering the extracellular potassium concentration in mouse cerebellar granule neurons. *J. Neurochem.* **68**, 750–759.

Pollegioni L, Sacchi S (2010) Metabolism of the neuromodulator D-serine. *Cell. Mol. Life Sci.* **67**, 2387–2404.

Ryder EF, Cepko CL (1994) Migration patterns of clonally related granule cells and their progenitors in the developing chick cerebellum. *Neuron* **12**, 1011–1028.

Sasabe J, Chiba T, Yamada M, Okamoto K, Nishimoto I, Matsuoka M, Aiso S (2007) D-serine is a key determinant of glutamate toxicity in amyotrophic lateral sclerosis. *EMBO J.* **26**, 4149–4159.

Shao Z, Kamboj A, Anderson CM (2009) Functional and immunocytochemical characterization of D-serine transporters in cortical and astrocytes cultures. *J. Neurosci. Res.* **87**, 2520–2530.

Shoji K, Mariotto S, Ciampa AR, Suzuki H (2006) Mutual regulation between serine and nitric oxide metabolism in human glioblastoma cells. *Neurosci. Lett.* **394**, 163–167.

Sikka P, Walker R, Cockayne R, Wood MJ, Harrison PJ, Burnet PW (2010) D-Serine metabolism in C6 glioma cells: involvement of alanine-serine-cysteine transporter (ASCT2) and serine racemase (SR) but not D-amino acid oxidase (DAO). *J. Neurosci. Res.* **88**, 1829–1840.

Stevens ER, Esguerra M, Kim PM, Newman EA, Snyder SH, Zahs KR, Miller RF (2003) D-Serine and serine racemase are present in the vertebrate retina and contribute to the physiological activation of NMDA receptors. *PNAS* **100**, 6789–6794.

Tay AS, Hu LF, Lu M, Wong PT, Bian JS (2010) Hydrogen sulfide protects neurons against hypoxic injury via stimulation of ATP-sensitive potassium channel/protein kinase C/extracellular signal-regulated kinase/heat shock protein 90 pathway. *Neuroscience* **167**, 277–286.

- Turpin FR, Potier B, Dulong JR, Sinet PM, Alliot J, Olier SH, Dutar P, Epelbaum J, Mothet JP, Billard JM (2011) Reduced serine racemase expression contributes to age-related deficits in hippocampal cognitive function. *Neurobiol Aging*, **32**, 1495–1504.
- Verrall L, Burnet PW, Betts JF, Harrison PJ (2010) The neurobiology of D-amino acid oxidase and its involvement in schizophrenia. *Mol. Psychiatry*, **15**, 122–137.
- Villalba M, Bockaert J, Journot L (1997) Concomitant induction of apoptosis and necrosis in cerebellar granule cells following serum and potassium withdrawal. *NeuroReport*, **8**, 981–985.
- Wu S, Barger SW (2004) Induction of serine racemase by inflammatory stimuli is dependent on AP-1. *Ann. N. Y. Acad. Sci.*, **1035**, 133–146.
- Xifro X, Malagelada C, Miñano A, Rodríguez-Alvarez J (2005) Brief exposure to NMDA produces long-term protection of cerebellar granule cells from apoptosis. *Eur. J. Neurosci.*, **21**, 827–840.
- Yuan Z, Gong S, Luo J, Zheng Z, Song B, Ma S, Guo J, Hu C, Thiel G, Vinson C, Hu CD, Wang Y, Li M (2009) Opposing roles for ATF2 and c-Fos in c-Jun-mediated neuronal apoptosis. *Mol. Cell. Biol.*, **29**, 2431–2442.
- Zhang FX, Rubin R, Rooney TA (1998) N-Methyl-D-aspartate inhibits apoptosis through activation of phosphatidylinositol 3-kinase in cerebellar granule neurons. A role for insulin receptor substrate-1 in the neurotrophic action of N-methyl-D-aspartate and its inhibition by ethanol. *J. Biol. Chem.*, **273**, 26596–26602.
- Zufferey R, Dull T, Mandel RJ, Bukovsky A, Quiroz D, Naldini L, Trono D (1998) Self-inactivating lentivirus vector for safe and efficient in vivo gene delivery. *J. Virol.*, **72**, 9873–9880.

Supporting Information

Additional supporting information may be found in the online version of this article:

Data S1 Procedures.

Fig. S1 Expression of D-serine racemase and D-serine in cerebellar granule neurons.

Fig. S2 Effect of KCl deprivation on SR expression in glial cells.

Fig. S3 Effect of D-JNK1-1 on CGNs apoptosis.

Fig. S4 Time course of P-Erk1-2 in Ad-LacZ and Ad-SR transduced neurons during apoptosis.

Fig. S5 Modulation of DAAO transcript levels and activity in CGNs undergoing apoptosis.

As a service to our authors and readers, this journal provides supporting information supplied by the authors. Such materials are peer-reviewed and may be re-organized for online delivery, but are not copy-edited or typeset. Technical support issues arising from supporting information (other than missing files) should be addressed to the authors.